Pyrolysis temperature affects phosphorus availability of rice straw and canola stalk biochars and biochar-amended soils

Caidi Yang[1,2] · Shenggao Lu[1,2]

Abstract

Purpose Biochars exhibited considerable differences in chemical properties with different feedstocks and pyrolysis conditions. This study was to understand the effects of pyrolysis temperature on the availability of phosphorus in biochars and biochar-amended soils.

Materials and methods Biochars from rice straw and canola stalk were produced at temperatures of 250, 350, 450, 550, and 650 °C, respectively, and then applied to two acidic soils (Ultisol and Alfisol). The availability of phosphorus in biochars and biochar-amended soils was evaluated.

Results The contents of total P and Olsen-P of biochar increased with pyrolysis temperature, reaching the maximum at 650 °C. The canola stalk biochar had a higher amount of total P than rice straw biochar. The addition of biochar increased the contents of total P, Olsen-P, and inorganic P (except Ca-P in Ultisol) in soils, varied with pyrolysis temperature, feedstock, and soil type. The highest phosphorous availability appeared in soils amended by biochars produced at 450 °C. The inorganic P in soils increased in the order of Ca-P > Fe–P > Al-P. Biochars significantly increased the contents of Al-P and Fe–P in two soils and Ca-P of Alfisol. Correlation analysis showed that there was a positive correlation between biochar pH and Olsen-P in soils, soil pH, and inorganic P.

Conclusions Biochar could largely affect the availability of phosphorus in soils. The amount and form of available P were dependent on pyrolysis temperature and feedstock. It was important to consider the most suitable pyrolysis temperature to improve the soil P availability better, which was essential to develop soil productivity on a large scale.

Keywords Biochar · Acidic soils · Pyrolysis temperature · Phosphorus availability · Inorganic P

1 Introduction

Phosphorus (P) is an essential element for plant growth and metabolism (Wang et al. 2014; Zhang et al. 2016). However, the low solubility of phosphates in soils makes it difficult for plants to use phosphates directly or indirectly (Ma et al. 2016; Shen et al. 2011). The deficiency of available P in soil has become one of the most important factors of limiting crop yields, especially in tropical and subtropical areas (Zhang et al. 2016; Blake et al. 2000). In order to cope with P deficiency in soil, it is necessary to activate P and provide available P for plant uptake. In recent years, the application of biochar has been considered as an effective amendment to provide the P nutrient and increase the availability of P in soil (Santos et al. 2019; Schneider and Haderlein 2016; Li et al. 2020).

Biochar is a product of thermal combustion of biomass feedstocks under anaerobic conditions at relatively low temperatures (300–700 °C) (Yang et al. 2020). The crop straw, as the largest agricultural biomass in subtropical area, has a huge potential as feedstocks for biochar production. The phosphorus in biomass feedstock almost completely retains in biochar in the pyrolysis process. Kim et al. (2018) found that the feedstocks with abundant P could generate the P-rich

✉ Shenggao Lu
lusg@zju.edu.cn

[1] Zhejiang Provincial Key Laboratory of Agricultural Resources and Environment, Zhejiang University, Hangzhou 310058, China

[2] College of Environmental and Resource Sciences, Zhejiang University, Hangzhou 310058, China

biochar. Gaskin et al. (2008) found that the mineral contents in biochar produced from different feedstocks increased in the order of poultry litters > herbs > woody plants. Therefore, the content of P in feedstock largely determines the content of P in biochar. In addition, the pyrolysis temperature of feedstock is another important parameter of affecting the nutrient contents of biochar (de Figueiredo et al. 2020; Hong and Lu 2018; Zhang et al. 2016). Previous studies indicated that the content of total P in the biochar increased with the pyrolysis temperature (Sun et al. 2018; Ahmad et al. 2012). When the pyrolysis temperature is above 700–800 °C, the P in biochar will lose and stabilize as insoluble forms. Besides, the duration time and heating rate of pyrolysis also affect the content and availability of P in biochar (Adhikari et al. 2019). Biochar is expected to act as a supply of available P when adding to the soil. To better manage the P nutrient in biochar, it is necessary to understand how the pyrolysis temperature affects the content and availability of P in biochar.

The addition of biochar contained a large amount of available P that supplies the exogenous P to the soil directly (Eduah et al. 2019; Dai et al. 2017). However, Yang et al. (2020) found that the increase of available P in the soil was mainly due to the endogenous P, which was activated by the addition of biochar. Biochar can increase the available P content in soil by promoting the dissolution of phosphate, which results from the change of soil chemical properties (Glaser et al. 2002; Chintala et al. 2014; Santos et al. 2019). It is concluded that the change of P availability in the biochar-amended soil is a comprehensive result of the increase of soil pH value, the increase of P saturation, and the strong interaction between P and biochar (Peng et al. 2021a; Morales et al. 2013). The effect of biochar on soil P availability varies with biochar feedstock, pyrolysis temperature, and soil types. A meta-analysis showed that the averaged relative change of soil available P with the addition of biochar with different feedstocks followed the order of the manure residue > crop residue > wood residue (Gao et al. 2019). Eduah et al. (2019) reported that biochar produced at 300–450 °C could effectively improve the bioavailability of P, especially in acidic soil. In acidic soils, the addition of biochar enhances P availability by reducing the adsorption of P on iron and aluminum oxides, which is because the increased pH induced by biochar leads to the precipitation of Fe^{3+} and Al^{3+} ions (Gérard 2016; Chintala et al. 2014; Hong and Lu 2018; Solaiman et al. 2019; Oladele et al. 2019). On the contrary, the addition of biochar increases the adsorption of P and reduces P availability in neutral or alkaline soils, which is due to a large number of cations (such as calcium and magnesium) that can complex with phosphate (Gustafsson et al. 2012; DeLuca et al. 2015; Harrington and Humphreys 2004).

Although there have been many studies on the content of P in biochars and their effect on the availability of P in soils, these results are not consistent (Yang et al. 2019; Peng et al.

2021b). For example, Parvage et al. (2013) found that the addition of wheat residue char had no effect, or even reduced the content of available P in soil. Thus, a more systematic research is needed to reveal how pyrolysis temperature and feedstock affect the availability of P in biochars and biochar-amended soils. In our study, the biochars were produced from two biomass feedstocks (rice straw and canola stalk) under five pyrolysis temperatures (250, 350, 450, 550, and 650 °C). The obtained biochars were applied to two soils (Ultisol and Alfisol) to investigate the effect of biochar on the availability of P in soil. The SEM–EDS observation was used to reveal the element distribution and binding state of biochar and soil mineral particles. The objectives of this study are to: (1) examine how the pyrolysis temperature and feedstock affect the availability of P in biochar, (2) compare the effects of biochar derived from different pyrolysis temperatures and feedstocks on the availability of P in biochar-amended soils, and (3) reveal the mechanisms of the influence of biochar on the availability of P in soil.

2 Materials and methods

2.1 Experimental materials

Rice straw (RS) and canola stalk (CS), the largest agricultural biomass in the subtropical region of China, were collected from Yueqing, Zhejiang Province, China. Rice straw was collected in November 2017 and canola stalk in May 2018. Both straws were cleaned with deionized water, dried at 105 °C for 24 h, and ground to pass a 2 mm sieve. Two soils (Ultisol and Alfisol) used in this study are the most representative agricultural soils in China. They were collected from the surface (0~20 cm) of soil. Ultisol was collected from the low-hilly region located in Yuyao (N29°45.6′, E121°07.2′), and Alfisol from paddy soil located in Dongyang, Zhejiang province (N29°17.4′, E120°14.4′), China. The basic properties of straws and soils are given in Table 1.

2.2 Biochar preparation and incubation experiment

Two straws (RS and CS) were placed in a separate porcelain crucible and covered tightly with a lid. The porcelain crucible was sealed with tin foil to keep out oxygen. Rice straw biochars (RB) and canola stalk biochars (CB) were produced under an anaerobic condition in a muffle furnace at 250, 350, 450, 550, and 650 °C, respectively. The heating rate was 10 °C min^{-1}, and after reaching the target temperature, samples were kept in the furnace for 2 h. Then the biochar was weighed to calculate the production yield and finely ground to pass 2-mm and 0.15-mm sieves, respectively. RB and CB produced at pyrolysis temperatures of 250, 350, 450, 550, and 650 °C were labeled

Table 1 Basic physicochemical properties of soil, straw, and biochars produced at different pyrolysis temperatures

Parameters	Yield (%)	pH	TOC (g kg^{-1})	Total K (g kg^{-1})	C (%)	H (%)	N (%)	S (%)	H/C	O/C
Ultisol	-	4.61	8.25	0.72	0.43	0.90	0.04	0.04	25.12	-
Alfisol	-	4.78	32.1	2.35	0.51	0.49	0.12	0.03	11.53	-
RS	-	8.93	289	10.6	37.8	5.13	1.09	0.11	1.63	0.54
RB250	65.4	7.64	418	18.8	45.1	4.62	0.86	0.28	1.23	0.32
RB350	41.9	9.94	420	36.1	48.7	3.55	0.91	0.26	0.87	0.29
RB450	34.6	10.6	519	38.8	50.4	2.75	0.83	0.27	0.65	0.28
RB550	31.2	11.1	423	40.6	48.5	2.08	0.77	0.24	0.51	0.29
RB650	8.76	11.2	394	54.2	39.8	1.73	0.71	0.36	0.52	0.37
CS	-	7.71	370	9.12	40.5	5.76	1.51	0.64	1.71	0.88
CB250	70.8	7.19	440	13.9	46.2	4.98	1.07	0.68	1.29	0.74
CB350	34.1	10.6	603	25.4	56.2	3.42	1.01	0.93	0.73	0.63
CB450	31.3	10.6	659	25.7	61.9	3.02	1.01	1.06	0.59	0.58
CB550	28.7	10.8	563	25.7	60.3	2.23	0.89	1.2	0.44	0.62
CB650	8.65	11.0	327	42.5	41.7	1.86	1.02	1.96	0.54	0.89

as RB250, RB350, RB450, RB550, RB650, CB250, CB350, CB450, CB550, and CB650, respectively.

The soils were air-dried at room temperature and then ground to pass a 2-mm sieve. The straws and biochars were thoroughly mixed with soils (Ultisol and Alfisol) with a proportion of 1% (w/w). Soils without straw or biochar were used as the control (CK). Each treatment was replicated three times. The straw/biochar-amended soils were packed into polyethylene cups with a bulk density of 1.2 g cm^{-3} by artificial compaction. The mixtures were wetted up to field water capacity using deionized water and incubated at constant temperature (25 °C). Soils were kept at constant moisture during the whole incubation process by adjusting the weight. After 90 days' incubation, soils were air-dried and ground to pass 2-mm and 0.15-mm sieves for further analyses.

2.3 Biochar and soil analyses

The pH of biochar and soil was determined by a pH meter (PB-21, Sartorius) with the suspension ratio of 1:20 and 1:2.5, respectively. Total organic carbon (TOC) was determined by oxidation method with potassium dichromate. Total potassium (TK) was determined by digesting biochar with $HClO_4$-HF solution and measured with a flame spectrophotometer (Bao 2000). The elemental composition (C, H, N, and S) of biochar and soil was determined, using an elemental analyzer (Elementar Analysensysteme GmbH, Germany). Around 1 mg of biochar samples was ground with 100 mg KBr for the preparation of pellets, and the IR spectra of samples were recorded in a wavenumber range of 4000–400 cm^{-1} by the Fourier-transform infrared spectroscopy (FTIR) (Shimadzu Ltd., Japan). The band assignments in the infrared spectra were done according to the literature

(Peng et al. 2011; Uchimiya et al. 2011). The X-ray diffraction (XRD) measurements were made using an X-ray diffractometer (Rigaku Corporation, Japan). The X-ray patterns were recorded in the range of $2\theta = 10$–$90°$ at a scan rate of $3°$ min^{-1}, with a generating voltage of 40 kV and a current of 40 mA. The morphology and chemical composition of samples were determined by using the scanning electron microscope (SEM) (SIRION-100; FEI, The Netherlands) with a dispersive spectrometer (EDS) (EDAX Co., USA), with the beam energy of 15 kV, a spot size of 3 mm, and a dwell time of 100 ms. The contents of oxygenic functional groups on the surface of biochar were determined by Boehm (1994) method. The Boehm titration method was used to conduct a qualitative and quantitative analysis of oxides according to the possibility of reaction between alkaline and acidic surface oxides with different strengths. Soil exchangeable acidity was extracted with KCl solution and determined by titration with NaOH (Bao 2000). Soil cation exchangeable capacity (CEC) was measured by ammonium acetate method, and the exchangeable base by atomic absorption spectrophotometer (exchangeable Ca^{2+} and Mg^{2+}) and a flame photometer (exchangeable K^+ and Na^+) (Bao 2000). The basic physicochemical properties of soil, straw, and biomass charcoal are shown in Table 1.

2.4 Phosphorus measurements of biochar and soil

The total P (TP) content of biochar and soil was determined, using the molybdate-ascorbic acid procedure after digesting samples with $HClO_4$-HF solution (Murphy and Riley 1962). The available P in biochar was extracted with deionized water, 0.5 M H_2SO_4 and 0.5 M $NaHCO_3$ (pH = 8.5) solution, respectively. Water-extractable P was readily plant-available P. The $NaHCO_3$-extractable P (Olsen-P) included

water-extractable P and labile P adsorbed on the surface of Fe and Al oxides or hydroxides or calcium carbonate. The sulfuric acid extracted readily plant-available P and available P in Ca, Fe, and Al phosphates (Mehlich 1978). The extractable P was determined by the phosphomolybdate colorimetric method. The P fractionation procedure modified from Hedley et al. (1982) was used to identify soil inorganic phosphates with different solubilities. In brief, soil samples were sequentially extracted by each of the following extractants: 1.0 M NH_4Cl for the loosely bound phosphate (NH_4Cl-P), 0.5 M NH_4F (pH 8.2) for the aluminum phosphate (Al-P), 0.1 M NaOH and 0.1 M Na_2CO_3 for the iron phosphate (Fe–P), and 0.5 M H_2SO_4 for the calcium phosphate (Ca-P). The concentrations of P in the extracts were immediately determined by the phosphomolybdate colorimetric method. All the extractions were repeated three times. The average data and standard deviations were reported.

2.5 Data analysis

SPSS 17.0 (SPSS, Inc., Chicago, IL, USA) was used for the statistical analysis of data. A one-way analysis of variance (ANOVA) was carried out to determine significant differences between treatments, using LSD's test with a significant level of $p < 0.05$. The Jupyter Lab of Python IDE was used for correlation characterization.

3 Results

3.1 Characterization of biochars

The characteristics of biochars produced at different pyrolysis temperatures are shown in Tables 1 and 2. Higher pyrolysis temperature resulted in higher pH in biochar, with a decreasing trend of production yield and H content. The CB had higher contents of C, N, and S than RB. The highest TOC was observed in biochar produced at 450 °C. The total oxygenic functional groups increased with the pyrolysis temperature,

which was 12.17 and 30.97 mmol g^{-1} for RB and CB at 650 °C, respectively. The content of acidic functional group decreased with the pyrolysis temperature, while the content of alkaline functional group increased. The pyrolysis temperature had no significant variation of carboxyl group in RB, while it affected the carboxyl group in CB significantly. Biochars produced at the temperature of 250 and 350 °C had more phenolic hydroxyl than the biochars produced at the relatively higher temperature, even though the content of phenolic hydroxyl was generally low in all the biochars. The spectral properties (FTIR) and X-ray diffraction (XRD) patterns are presented in Figs. S1 and S2. Adsorption intensities at the bands of 3400 and 2900 cm^{-1} decreased with the pyrolysis temperature, indicating the reduction of O–H and aliphatic C–H bonds. The intensified adsorption at 1400 cm^1 indicated the increase of aromatic C. The visible peaks at 3407, 2923, 1630, 1578, 1422, and 1055 cm^{-1} indicated that the considerable amounts of original organic residues were preserved at 450 °C, whereas most of them disappeared at 650 °C. Some visible peaks at 1000–600 cm^{-1} could be assigned to the metal–oxygen bonds. The main mineral types of biochar were quartz, sylvite, phosphate, and calcite; in addition to this, the RB included arcanite, while CB included halite. There was a trend for the intensity and peak value to increase with the pyrolysis temperature, implying that the carbonization may form some minerals or change some crystalline phases and mineral compositions.

### 3.2 Content of total P and available P in biochars

The effects of pyrolysis temperature and feedstock on the content of total P and available P in biochars are shown in Fig. 1. The amount of total P and Olsen-P in biochars significantly ($p < 0.05$) increased with the pyrolysis temperature. The contents of total P in RB650 and CB650 were as high as 3.94 and 5.06 g kg^{-1}, and Olsen-P 1.09 and 1.18 g kg^{-1}, respectively. There was no significant difference in the content of Olsen-P between the rice straw and canola stalk biochars. Pyrolysis temperature had no significant effect on

Table 2 The change of surface oxygenic functional groups (alkali, acid, carboxyl, and phenol) of biochars (RB and CB) with different pyrolysis temperatures

Biochars	Alkali (mmol g^{-1})	Acid (mmol g^{-1})	Carboxyl (mmol g^{-1})	Phenol (mmol g^{-1})
RB250	5.94 ± 0.15c	6.15 ± 0.11a	5.70 ± 0.15a	0.36 ± 0.03a
RB350	6.18 ± 0.24b	5.97 ± 0.09b	5.49 ± 0.09ab	0.15 ± 0.01b
RB450	6.23 ± 0.06b	5.67 ± 0.07c	5.45 ± 0.02b	0.08 ± 0.01c
RB550	6.45 ± 0.11a	5.47 ± 0.08d	5.38 ± 0.15b	0.03 ± 0.00d
RB650	6.49 ± 0.08a	5.40 ± 0.07e	5.59 ± 0.10ab	0.09 ± 0.03c
CB250	13.6 ± 0.05e	14.6 ± 0.11b	13.3 ± 0.21d	1.42 ± 0.04a
CB350	14.0 ± 0.07d	15.2 ± 0.01a	13.7 ± 0.04c	1.67 ± 0.07b
CB450	14.4 ± 0.12c	14.1 ± 0.07c	14.5 ± 0.11b	0.96 ± 0.05d
CB550	15.7 ± 0.16b	14.2 ± 0.08c	15.0 ± 0.11a	0.60 ± 0.05e
CB650	16.0 ± 0.05a	14.0 ± 0.55c	14.0 ± 0.02c	1.25 ± 0.03c

Different letters indicate significant difference between treatments ($p < 0.05$, LSD test)

Fig. 1 Changes of total P, Olsen-P, H_2O-, and H_2SO_4-extractable P of biochars (RB and CB) with different pyrolysis temperatures. Error bars indicate ± standard deviation. Different letters above error bars indicate significant difference between treatments ($p < 0.05$, LSD test)
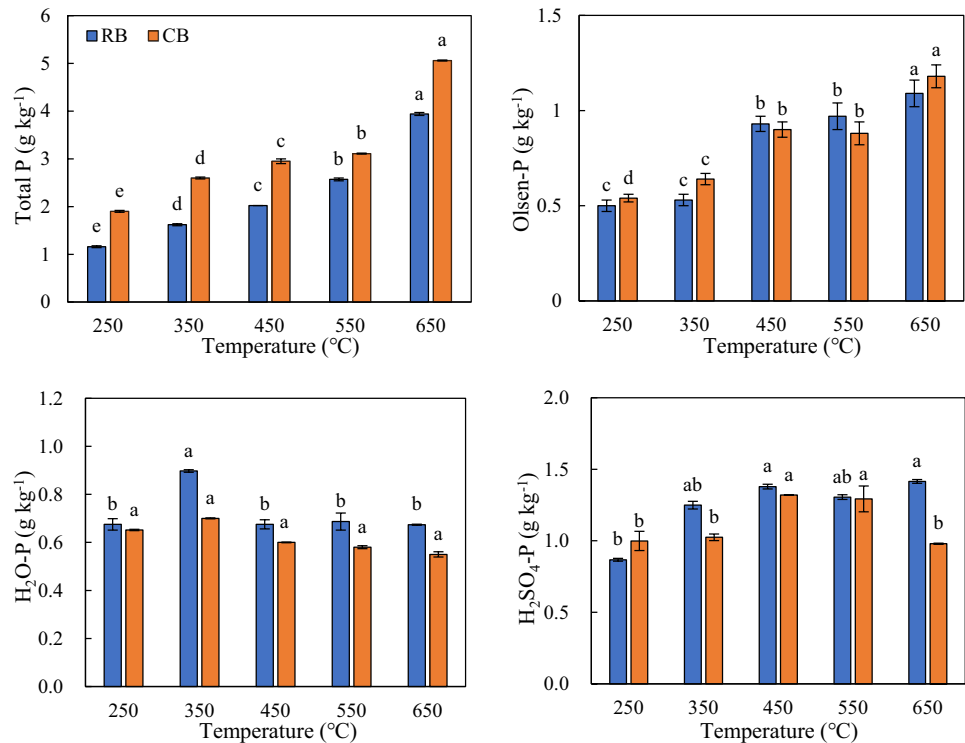
the contents of H_2O-P and H_2SO_4-P in the biochar. At the same pyrolysis temperature, the content of total P in CB was higher than that of RB, while the H_2O-P exhibited an opposite trend. The RB had higher content of H_2SO_4-P than the CB at the temperature above 250 °C. Among the tested extract solutions, the amount of H_2SO_4-extractable P in rice straw biochar was much higher than either H_2O-P or Olsen-P, which followed in the order of H_2SO_4-P > Olsen-P > H_2O-P.

3.3 The acidity, SOM, and exchange cations in biochar-amended soils

The effects of biochars produced with different pyrolysis temperatures and feedstocks on soil properties are shown in Table 3. Compared with the straw, biochar had a greater impact on the soil acidity, soil organic matter (SOM), and exchange cation composition. The addition of straw and biochar increased the pH of the soil. For the Ultisol, both RS and RB significantly ($p < 0.05$) increased the pH by 0.23–0.37 units, and CS and CB produced at the pyrolysis of 250–450 °C significantly increased the soil pH. On the contrary, the addition of straw and biochar significantly ($p < 0.05$) decreased the exchangeable acid content. For the Alfisol, the addition of biochar had no significant effect on the exchangeable acid content because of its relatively high organic matter. The original SOM values of the Ultisol and Alfisol were 8.25 and 22.77 g kg^{-1}, which significantly ($p < 0.05$) increased by 67.7–173% and 36.6–63.9%, with the addition of straws and biochars,

respectively. The content of SOM in soils treated with biochars was higher than the straw-treated soils. The soils treated with biochar produced at the temperature of 550 °C had the largest content of organic matter. The content of exchangeable cations in Ultisol increased with the pyrolysis temperature between 250 and 550 °C. The addition of biochar significantly increased the CEC of both soils. The largest increases of CEC in two soils were observed in the CB450 treatment, which increased by 42.0% for Ultisol and 48.1% for Alfisol, respectively. The largest contents of exchangeable Ca^{2+} and Na$^+$ were also found in the Ultisol treated with the canola stalk biochar, produced at the temperature of 450 °C. On the other hand, the effect of biochar on soil CEC also depended on soil types (Table 3). The CB increased the CEC of Ultisol more than the Alfisol, while RB increased the exchangeable Ca^{2+} and Mg^{2+} of the Alfisol more than the Ultisol.

3.4 Content of available P in biochar-amended soils

The effects of biochars prepared at different pyrolysis temperatures on the total and available P in soils are shown in Fig. 2. The content of total P in biochar-amended soils was significantly higher than the control. The soils treated with the RB450 and CB550 had much higher values of total P, which were 0.74 and 0.67 g kg^{-1} for the Ultisol and 1.37 and 1.57 g kg^{-1} for the Alfisol, respectively. The contents of available P extracted by different extraction methods followed the order of Olsen-P > H_2SO_4-P > H_2O-P, which were higher in

Table 3 Effects of biochar produced at different pyrolysis temperatures on the acidity, SOM, and cation exchange performance of two soils (Ultisol and Alfisol)

Treatments	pH	Exchangeable acid (cmol kg^{-1})	SOM (g kg^{-1})	CEC (cmol kg^{-1})	K$^+$ (cmol kg^{-1})	Ca^{2+} (cmol kg^{-1})	Na$^+$ (cmol kg^{-1})	Mg^{2+} (cmol kg^{-1})
Soil type	Ultisol							
CK	4.61 ± 0.11f	7.79 ± 0.10a	8.25 ± 0.58f	13.25 ± 0.59d	1.03 ± 0.11e	2.38 ± 0.20c	1.01 ± 0.13d	1.03 ± 0.15e
RS	4.84 ± 0.01d	5.80 ± 0.20c	14.14 ± 0.56e	13.72 ± 0.43 cd	1.77 ± 0.18d	2.58 ± 0.09c	1.25 ± 0.12d	2.32 ± 0.04b
RB250	4.89 ± 0.01 cd	5.20 ± 0.24e	13.83 ± 0.63e	13.81 ± 0.87 cd	1.73 ± 0.12d	2.79 ± 0.03b	1.78 ± 0.69c	2.30 ± 0.03b
RB350	4.96 ± 0.01bc	6.15 ± 0.60bc	18.73 ± 1.72c	15.68 ± 0.28bc	3.01 ± 0.08c	2.71 ± 0.09b	1.51 ± 0.05c	2.30 ± 0.06b
RB450	4.94 ± 0.02bc	5.50 ± 0.17d	21.69 ± 2.78ab	15.31 ± 0.41bc	3.05 ± 0.25c	2.99 ± 0.03b	1.26 ± 0.05d	2.51 ± 0.08a
RB550	4.98 ± 0.03bc	5.00 ± 0.18f	22.51 ± 1.18a	16.18 ± 0.24b	3.86 ± 0.14b	2.94 ± 0.08b	1.88 ± 0.01c	2.50 ± 0.01a
RB650	4.89 ± 0.04 cd	5.18 ± 0.04e	19.23 ± 0.04b	15.46 ± 0.31bc	3.02 ± 0.01c	2.98 ± 0.12b	1.74 ± 0.19c	2.53 ± 0.01a
CS	4.71 ± 0.01e	6.21 ± 0.07b	14.60 ± 1.30e	14.48 ± 0.12c	1.92 ± 0.04d	2.74 ± 0.03b	1.49 ± 0.03c	2.12 ± 0.02c
CB250	5.02 ± 0.02b	5.76 ± 0.30c	15.40 ± 0.47de	16.83 ± 0.47ab	2.24 ± 0.07d	2.93 ± 0.03b	3.77 ± 0.36b	2.14 ± 0.01c
CB350	4.96 ± 0.02bc	4.69 ± 0.25f	15.91 ± 0.57d	16.97 ± 0.61ab	3.30 ± 0.47c	3.21 ± 0.01ab	3.50 ± 0.12b	2.28 ± 0.01b
CB450	5.20 ± 0.00a	4.34 ± 0.13 g	19.67 ± 0.98ab	18.92 ± 0.55a	3.09 ± 0.13c	3.43 ± 0.06a	5.99 ± 0.30a	2.06 ± 0.06c
CB550	4.72 ± 0.05e	4.83 ± 0.20f	21.04 ± 1.07ab	17.88 ± 0.86a	5.68 ± 0.47a	2.71 ± 0.02b	2.98 ± 0.29bc	1.69 ± 0.08d
CB650	4.60 ± 0.07f	4.50 ± 0.07f	19.28 ± 0.40b	15.33 ± 0.51bc	4.04 ± 0.21b	2.85 ± 0.11b	2.73 ± 0.08bc	1.21 ± 0.11e
Soil type	Alfisol							
CK	5.07 ± 0.15 cd	0.70 ± 0.30ab	22.77 ± 0.88d	15.73 ± 0.58d	0.40 ± 0.12e	9.94 ± 0.33d	1.74 ± 0.11e	2.96 ± 0.18d
RS	5.13 ± 0.14c	0.70 ± 0.05ab	31.10 ± 3.28bc	19.61 ± 1.64 cd	2.37 ± 0.65c	10.86 ± 0.39b	1.77 ± 0.47e	3.93 ± 0.13a
RB250	5.12 ± 0.10c	0.55 ± 0.05b	34.76 ± 0.62b	20.17 ± 0.36c	2.46 ± 0.08c	10.90 ± 0.08b	2.20 ± 0.16d	4.05 ± 0.04a
RB350	5.25 ± 0.13b	0.55 ± 0.15b	35.06 ± 1.90b	20.85 ± 0.27bc	3.39 ± 0.11b	10.58 ± 0.11bc	2.53 ± 0.01d	3.79 ± 0.04ab
RB450	5.37 ± 0.13a	0.55 ± 0.02b	35.79 ± 0.26b	21.10 ± 0.80b	3.03 ± 0.31b	11.26 ± 0.32a	2.38 ± 0.09d	3.88 ± 0.08a
RB550	5.25 ± 0.01b	0.22 ± 0.13c	36.30 ± 1.42ab	20.09 ± 1.37c	2.83 ± 1.11bc	10.74 ± 0.18b	2.54 ± 0.05d	3.76 ± 0.03ab
RB650	5.44 ± 0.07a	0.43 ± 0.00bc	36.32 ± 0.06ab	21.56 ± 0.49b	3.86 ± 0.23a	11.04 ± 0.07a	2.45 ± 0.15d	3.77 ± 0.04ab
CS	5.03 ± 0.04d	0.60 ± 0.05ab	35.17 ± 3.16b	20.08 ± 0.63c	2.22 ± 0.17c	11.05 ± 0.19a	2.66 ± 0.22d	3.56 ± 0.05b
CB250	5.07 ± 0.10 cd	0.75 ± 0.05ab	30.33 ± 0.85c	21.14 ± 0.45b	1.88 ± 0.26d	11.20 ± 0.15a	3.78 ± 0.02bc	3.54 ± 0.02b
CB350	5.15 ± 0.08c	0.45 ± 0.10b	34.08 ± 2.12b	20.82 ± 0.50bc	2.62 ± 0.07bc	10.20 ± 0.33 cd	4.28 ± 0.06b	3.27 ± 0.04c
CB450	5.35 ± 0.21a	0.80 ± 0.00a	37.10 ± 0.15a	23.33 ± 0.54a	2.28 ± 0.23c	10.34 ± 0.19c	6.65 ± 0.03a	3.26 ± 0.09c
CB550	5.27 ± 0.18b	0.80 ± 0.00a	37.33 ± 2.12a	21.40 ± 0.12b	3.71 ± 0.05a	10.44 ± 0.04c	3.27 ± 0.02c	3.17 ± 0.01 cd
CB650	5.11 ± 0.03c	0.60 ± 0.03ab	35.96 ± 2.39ab	21.14 ± 0.39b	3.93 ± 0.08a	10.32 ± 0.13c	3.19 ± 0.12c	3.10 ± 0.06d

Different letters indicate significant difference between treatments ($p < 0.05$, LSD test)

the Alfisol than the Ultisol. Biochar-amended soils had higher content of available P than the straw-amended soils. All biochar treatments significantly increased the content of Olsen-P in the Ultisol. The maximum contents of Olsen-P in the Alfisol were observed in the RB450 and CB450 treatments, respectively. The RB450 and CB450 treatments increased the content of Olsen-P by 115 and 110% for Ultisol and 149 and 170% for Alfisol, respectively, compared to the control. All treatments had no significant impact on the H_2O-extrable P content of the Ultisol, but significantly increased the H_2O-extractable P content of the Alfisol. The H_2O-extractable P contents of the Alfisol were 2.12 and 1.73 mg kg^{-1} under RB450 and CB450 treatments, increasing by 105% and 68.0%, respectively. The effect of biochar treatments on the H_2SO_4-extractable content of two soils was consistent with the change of Olsen-P. The soils treated with RB450 and CB450 had the maximum content of H_2SO_4-extractable P,

which increased by 94.5% and 110% for Ultisol and 18.4% and 17.7% for Alfisol, respectively, compared to the control.

3.5 Inorganic P in biochar-amended soils

The effects of biochars prepared at different pyrolysis temperatures on the soil inorganic P are shown in Fig. 3. The contents of various inorganic P in soils followed the order of Ca-P > Fe–P > Al-P. The biochar-amended soils had more inorganic P than straw-treated soils. However, the effect of biochar on the inorganic P in the soils varied with the pyrolysis temperature and the feedstock type. The rice straw biochar significantly ($p < 0.05$) increased the contents of Al-P and Fe–P, while it decreased the content of Ca-P in the Ultisol. The CB450 treatment significantly increased the contents of Al-P and Fe–P, while it had no significant effect on the content of Ca-P in the Ultisol.
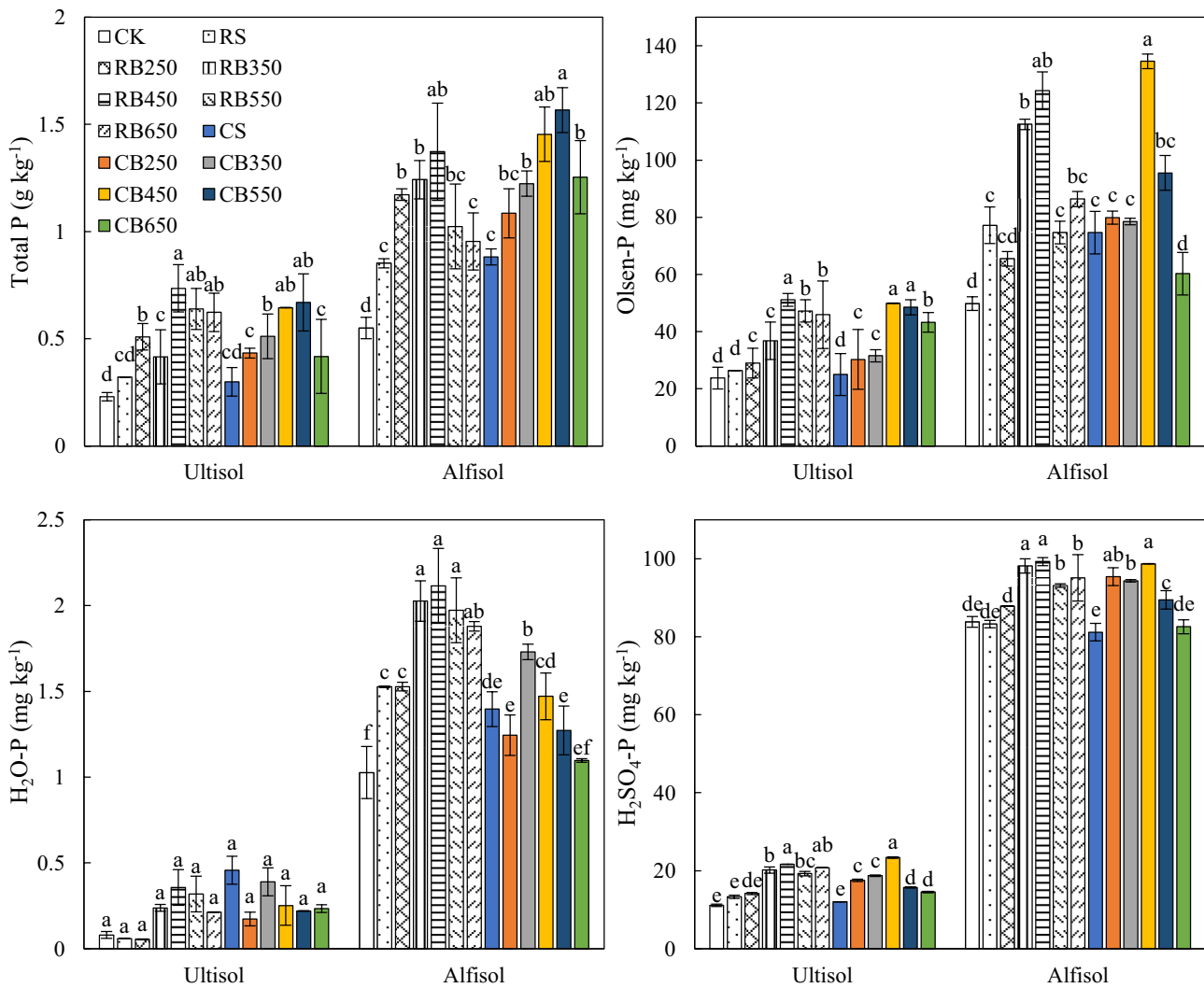
Fig. 2 The total P, Olsen-P, H$_2$O-, and H$_2$SO$_4$-extractable P of two soils (Ultisol and Alfisol) amended with biochars produced in the different pyrolysis temperatures. Error bars indicate ± standard devia-tion. Different letters above error bars indicate significant difference between treatments ($p < 0.05$, LSD test)

For the biochar-amended Alfisol, only RB450 and CB450 treatments significantly increased the contents of Al-P and Ca-P. Under RB450 and CB450 treatments, the content of Al-P increased by 124% and 190% in the Ultisol and 55.2% and 42.4% in the Alfisol, and the content of Fe–P increased by 61.4% and 72.1% in the Ultisol and 23.8% and 16.2% in the Alfisol, respectively, compared to the control. RB450 and CB450 treatments increased the Ca-P contents in the Alfisol by 26.5% and 32.5%, respectively. Therefore, the RB450 treatment had the largest effect on increasing the contents of Al-P and Fe–P in the Alfisol, while the CB450 treatment had the largest effect on increasing Al-P and Fe–P in the Ultisol and Ca-P in the Alfisol.

3.6 SEM–EDS observation on biochar-amended soils

Our results indicated that biochar made at 450 °C had the largest effect on the availability of P and inorganic P forms in soils. Thus, the soils treated by RB450 and CB450 were observed and their SEM images and EDS spectra are shown in Fig. 4. SEM images (A, B, C, and D) of biochar-treated soils showed that soil mineral particles were not only attached to the surface of biochar (sites b, e, h, and k), but also entered into the pores of biochar (sites e, f, i, and l). The EDS maps of biochar-treated soils showed that biochar was almost composed of C element, while soil mineral particles
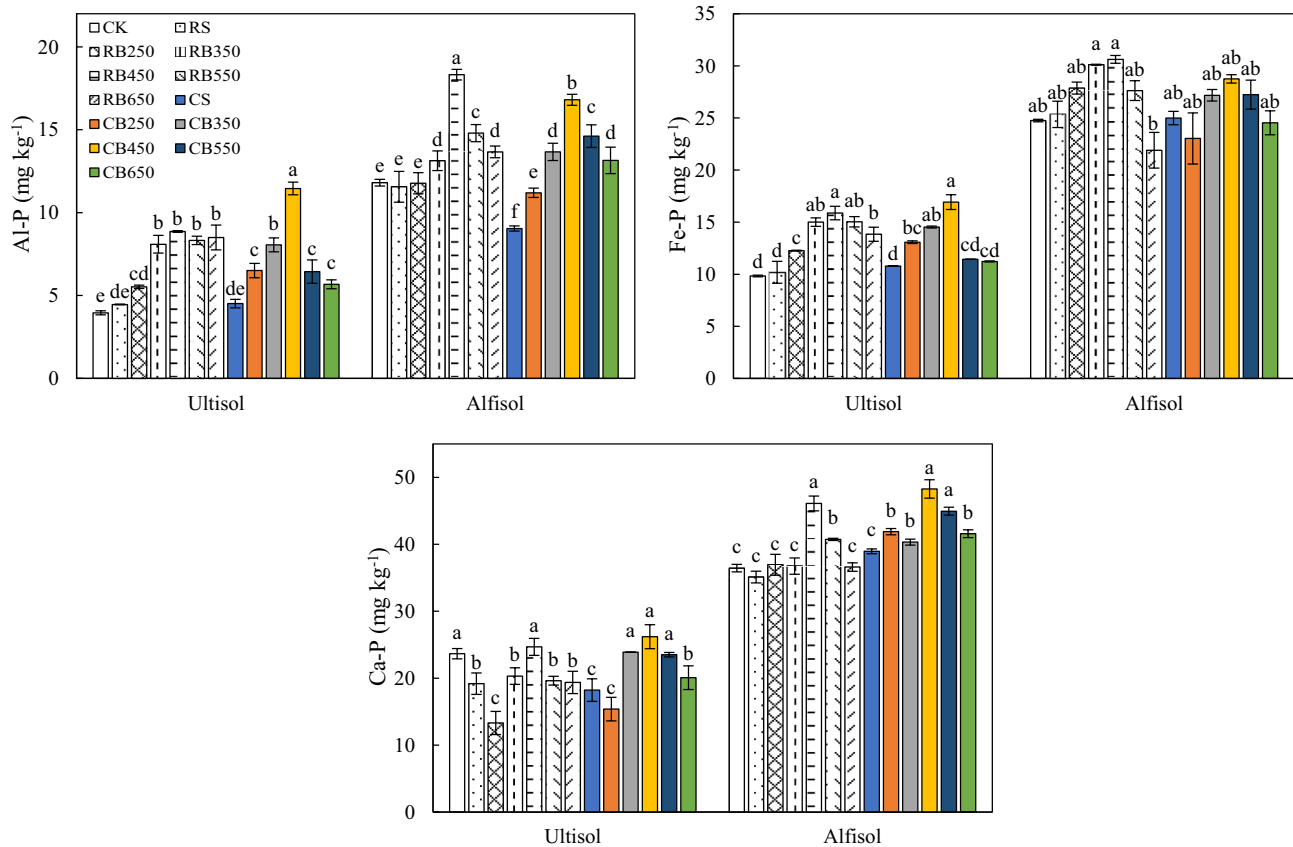
Fig. 3 The content of inorganic P in the soils (Ultisol and Alfisol) amended with biochars produced in different pyrolysis temperatures. Error bars indicate ± standard deviation. Different letters above error bars indicate significant difference between treatments ($p < 0.05$, LSD test)

were mainly composed of Si and Al elements, indicating the distribution and binding state of biochar and soil particles. The characterization of P on biochar (site j) indicated that the P contained in biochar could be released into the soil directly. Meanwhile, fine mineral particles could be inserted into the pores of biochar and produced aggregation effect in the biochar-amended soils. These interactions promoted the release and conversion of P in both biochar and soil mineral particles.

4 Discussion

4.1 Effect of pyrolysis temperature on P availability in biochar

Our results indicated that the pyrolysis temperature and feedstock type, as the important factors in determining the potential application of biochar, could largely affect the contents of total P and available P in biochar. On the whole, the total P and Olsen-P in biochar were positively correlated with the pyrolysis temperature due to the C volatilization and P preservation. The higher temperature

yielded the greater decomposition of biomass structure, which resulted in higher residual phosphate (Figueiredo et al. 2018). The correlation analysis showed that there were significant positive correlations between pyrolysis temperatures and total-P ($R^2 = 0.86$, $p < 0.01$) and Olsen-P ($R^2 = 0.95$, $p < 0.01$) of biochar (Table 4). Studies have shown that K and P were lost at above 800 °C, while Mg and Ca at above 1200 °C. Therefore, the enrichment of the base cations and P with the pyrolysis temperature was due to their higher vaporization energy (Dai et al. 2017; Knicker 2007; Zheng et al. 2013). The IR spectra revealed that the functional groups in the biochar decreased with the pyrolysis temperature while the carbonization had an opposite trend due to the loss of oxygen-containing species (Ahmad et al. 2012). The XRD patterns also showed that there were more calcite and phosphate at the higher pyrolysis temperature (Fig. S2). Qian and Jiang (2014) found that P could transfer to available form with the increasing pyrolysis temperature, especially from 400 to 500 °C. Uzoma et al. (2011) reported that the content of Olsen-P in a woody biochar produced at 500 °C was as high as 23 g kg^{-1}, while the Olsen-P in the biochar produced at 300 °C was only 1.2 g kg^{-1}.
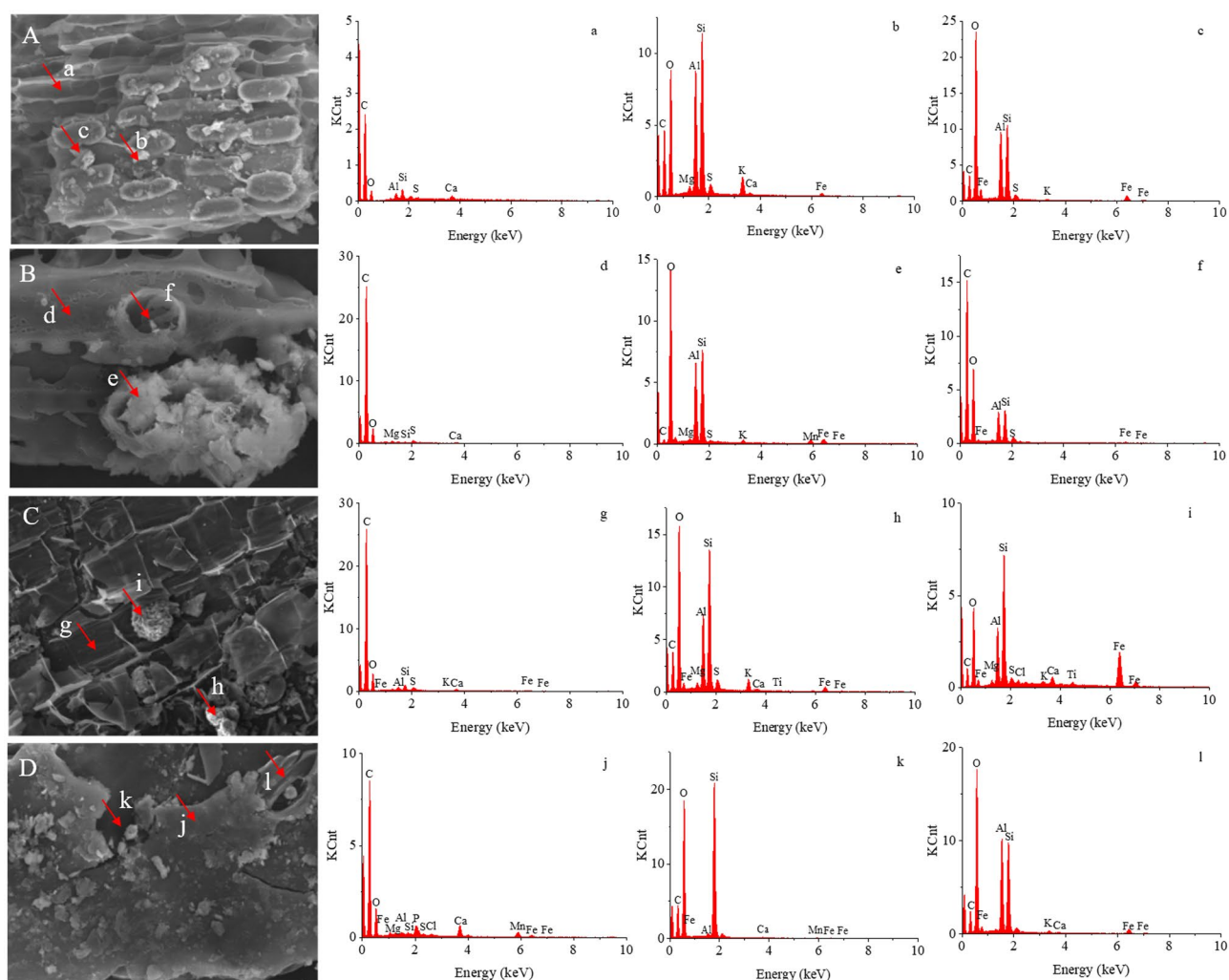
Fig. 4 SEM images and EDS maps of soils amended with biochars produced at pyrolysis temperature of 450 °C. **A** Ultisol + RB; **B** Ultisol + CB; **C** Alfisol RB; **D** Alfisol CB. The lowercase letters "**a**" to "**l**" represent the site of EDS

The main form of P in biochar was solid phosphate. Therefore, the release of soluble P in biochar was mainly regulated by the dissolution reaction, which was significantly affected by the pH value of the solution (Liu et al. 2018; Wei et al. 2013; da Silva and Fitzsimmons 2016). The pH of biochar increased with the pyrolysis temperature because of the separation of alkali salt from the biomass structure and the increase of alkaline functional groups on the surface of biochar (Ahmad et al. 2012; Kameyama et al. 2012). In addition, the cations in straw were pyrolyzed to form carbonate or oxide. The pH of biochar played an important role in P complexation, dissolution, and precipitation. The correlations showed that there were significant positive correlations between pH of biochar and total-P ($R^2 = 0.63$, $p < 0.05$) and Olsen-P ($R^2 = 0.77$, $p < 0.01$) (Table 4). However, the water- and H_2SO_4-extractable P had no significant correlations with the total P in the biochar. Among the three extraction methods, Olsen-P extraction was buffered at a pH of 8.5, H_2SO_4 extraction was strongly acidic, and water extraction depended upon the pH of biochar. The weak correlation between water-extractable P and total P in the biochar could be explained by the variations of pH in biochar. Studies have shown that the phosphate could be adsorbed on the surface of biochar by anion exchange, which was closely related to basic functional groups in biochar. In addition, the surface deposition of phosphate on metal oxides (such as MgO, Al_2O_3, and CaO) of biochar surface was also a potential mechanism for biochar adsorption of PO_4^{3-} (Hollister et al. 2013; Wang et al. 2015). The phosphate extracted by water was easily-soluble P in biochar and H_2SO_4-extractable P was the slow-soluble P, consisting of P binding Ca (mostly), Mg, and other elements. The increase of H_2SO_4-P in biochar was due to the enhanced contact between Ca, Mg, and P after the conversion of organic matter in straw and then the

Table 4 Correlation coefficients between biochar properties and soil acidity and P fractionations. Superscripts 1 and 2 represent the biochar and soil properties, respectively. EX, exchangeable. **Correlation is significant at the 0.01 level, *Correlation is significant at the 0.05 level. The lower left corner represents the correlation of Ultisol, and the upper right corner represents the correlation of Alfisol

Parameters	TP	pH¹	TOC¹	TP¹	Olsen-P¹	H₂O-P¹	H₂SO₄-P¹	PH²	EX-Acid²	SOM²	TP²	Olsen-P²	H₂O-P²	H₂SO₄-P²	Al-P²	Fe-P²	Ca-P²
TP	1	0.82**	-0.22	0.86**	0.95**	-0.43	0.10	0.62	-0.21	0.70*	0.00	-0.06	-0.02	-0.30	0.36	-0.29	0.14
pH¹	0.82**	1	0.17	0.63*	0.77**	-0.13	0.33	0.77**	-0.32	0.78**	0.19	0.25	0.31	0.04	0.63	0.14	0.24
TOC¹	-0.22	0.17	1	-0.21	-0.16	-0.14	0.66*	0.30	0.39	0.19	0.63	0.62	0.03	0.49	0.54	0.44	0.66*
TP¹	0.86**	0.63*	-0.21	1	0.85**	-0.60	-0.09	0.38	0.02	0.42	0.01	-0.23	-0.39	-0.47	0.10	-0.53	0.15
Olsen-P¹	0.95**	0.77**	-0.16	0.85**	1	-0.57	0.15	0.57	-0.16	0.64*	0.03	-0.00	-0.06	-0.25	0.48	-0.27	0.31
H₂O-P¹	-0.43	-0.13	-0.14	-0.60	-0.57	1	0.03	0.05	-0.38	-0.21	-0.29	0.22	0.71*	0.52	-0.14	0.41	-0.56
H₂SO₄-P¹	0.10	0.33	0.66*	-0.09	0.15	0.03	1	0.65*	0.21	0.43	0.31	0.83**	0.31	0.71*	0.66*	0.32	0.51
PH²	-0.48	-0.20	0.54	-0.54	-0.39	0.33	0.71*	1	-0.11	0.51	0.09	0.58	0.45	0.54	0.63*	0.00	0.28
EX-Acid²	-0.47	-0.47	-0.37	-0.62	-0.55	0.76*	-0.16	0.15	1	-0.10	0.69*	0.38	-0.65*	-0.00	0.01	-0.00	0.54
SOM²	0.72*	0.78**	0.08	0.38	0.71*	-0.12	0.43	-0.10	-0.16	1	0.41	0.31	0.19	-0.11	0.61	0.33	0.26
TP²	0.379	0.49	0.49	0.01	0.44	-0.27	0.64*	0.21	-0.27	0.65*	1	0.54	-0.28	0.01	0.50	0.56	0.72*
Olsen-P²	0.75*	0.77**	0.22	0.46	0.79**	-0.34	0.58	-0.04	-0.35	0.92**	0.77**	1	0.39	0.79**	0.73*	0.58	0.57
H₂O-P²	0.27	0.67*	0.41	0.17	0.31	0.11	0.23	0.16	-0.17	0.54	0.36	0.41	1	0.65*	0.43	0.47	-0.25
H₂SO₄-P²	0.08	0.39	0.47	-0.10	0.15	0.30	0.83**	0.74*	0.09	0.42	0.48	0.48	0.53	1	0.47	0.36	0.22
Al-P²	0.12	0.45	0.61	-0.02	0.20	0.14	0.91**	0.75*	-0.17	0.42	0.52	0.53	0.51	0.95**	1	0.56	0.71*
Fe-P²	-0.14	0.26	0.51	-0.31	-0.04	0.40	0.76*	0.84**	0.09	0.30	0.41	0.32	0.54	0.93**	0.92**	1	0.31
Ca-P²	0.37	0.74*	0.71*	0.30	0.41	-0.14	0.59	0.17	-0.43	0.61	0.56	0.67*	0.75*	0.59	0.68*	0.52	1

dissolution of insoluble Ca-P and Mg-P compounds (Cross and Schlesinger 1995). Therefore, straw biochar could function as a reservoir of P and an important resource of releasing available P. The potential available P in biochar could be extracted by NaHCO$_3$-and H$_2$SO$_4$ solutions.

4.2 Effect of pyrolysis temperature on P availability in biochar-amended soils

The incubation experiment indicated that the application of biochar could effectively affect the P availability in soil, especially the Ultisol. The increased contents of total-P, available P, and inorganic P in biochar-amended soils were

partly due to the direct diffusion of available P in biochar, and partly due to the change of soil physical and chemical properties, which further affected the P availability in soils. The addition of biochars was able to bring available P into soils, but the amount and form of available P were dependent on pyrolysis temperature and feedstock type. The result was consistent with many previous studies (Cole et al. 2019; Gao and DeLuca 2018; Hong and Lu 2018). A meta-study on the effect of biochar amendment on the P availability of various soils around the world showed that application of biochar was able to increase plant-available P in neutral (pH 6.5–7.5) and acidic soils (pH < 6.5), while they found no positive effects on P availability in alkaline soils (Glaser and
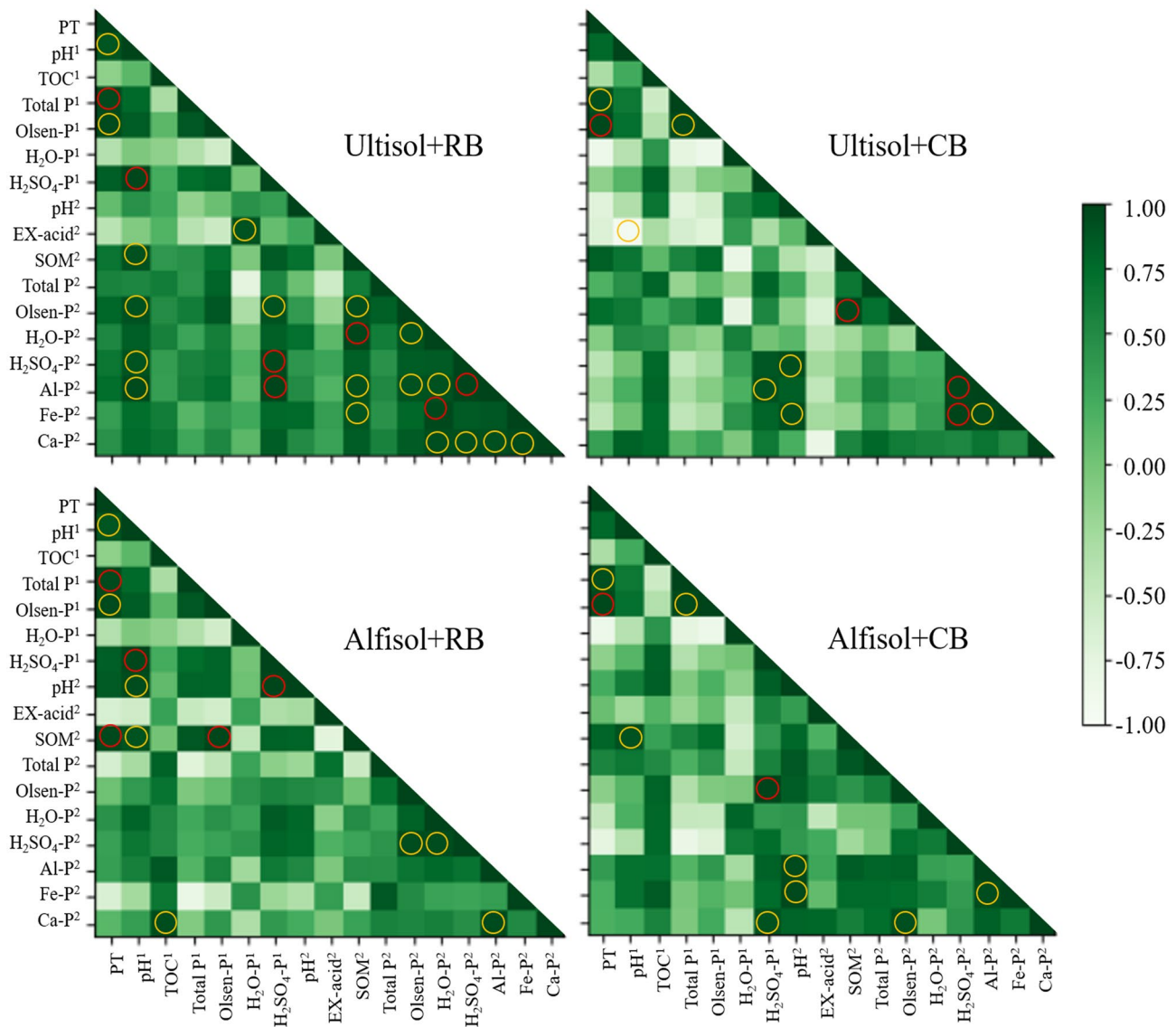

Fig. 5 Correlation comparison of P availability of biochars and biochar amended soils among different feedstocks and soil types. Superscripts 1 and 2 represent properties of biochars and soils, respectively. PT, pyrolysis temperature; EX, exchangeable. The darker color represents the higher positive correlation (close to 1); the lighter color represents the higher negative correlation (close to -1). Red circles indicate significant correlation at the level of 0.01, while yellow circles indicate at the level of 0.05

Lehr 2019). The soil pH was considered as one of the major factors in affecting the bioavailability and transformation of P in soil. The application of biochar indirectly changed the P availability by affecting soil pH (Gustafsson et al. 2012). The maximum availability of P in soil was recorded at the pH range of 5.5–7.2. The application of biochar to acidic soil increased the soil pH and then led to the precipitation of polymeric Fe and Al oxides, thereby increasing the availability of P in soil. In addition, the increased pH could dissolve the phosphates bound with Fe^{3+} and Al^{3+} ions and released available P (da Silva and Fitzsimmons 2016; Gérard 2016). Morales et al. (2013) also found that biochar reduced the fixed capacity of P in degraded acidic tropical soils. Higher pyrolysis temperature could enhance the availability of phosphate in biochar-amended soils because of the higher biochar pH. The correlations between the properties of biochar and soil showed that there were positive correlations between biochar pH and Olsen-P ($R^2 = 0.77$, $p < 0.01$) in two soils (Table 4). The soil pH was positively correlated with the Al-P ($R^2 = 0.75$, $p < 0.05$), Fe–P ($R^2 = 0.84$ $p < 0.01$) of the Ultisol and the Al-P ($R^2 = 0.63$ $p < 0.01$) of the Alfisol (Table 4). The soil organic matter (SOM) was another important factor affecting the availability and forms of phosphate in soil. The SOM would provide a good environment for the survival and metabolism of soil microorganisms and promote the activities of P-solubilizing microbes (Xu et al. 2016). The correlation analysis showed that there were positive correlations between SOM and total-P ($R^2 = 0.65$, $p < 0.05$), Olsen-P ($R^2 = 0.92$, $p < 0.01$) of Ultisol (Table 4). Biochar had a more noticeable effect on the contents of Al-P and Fe–P in soil, which could be explained by the changes in pH and other chemical properties in acidic soil. The changes of soil chemical environment could affect the binding state of iron, aluminum, and other metals with P and then promote the release of P from precipitates. The OH– had a desorption effect on adsorbed iron P, thus significantly increasing the content of Fe–P (Hass et al. 2012). Thus, the impacts of biochar on P availability in soil were regulated by changes of soil chemical properties, specifically soil pH.

The pyrolysis temperature of biochar also largely influenced the content of available P and chemical forms of P in biochar-amended soil. The effect of biochar produced at the lower temperature on the availability of P in soil was not obvious, which was due to the low decomposition degree of soluble phosphate. The increasing temperatures could result in higher proportion of available P and pH value in biochar because of the higher decomposition degree of biomass feedstock. Another potential mechanism was related to porous structure of biochar produced at higher temperature. The porous biochar could be the good habitat for microorganism such as P solubilizing bacteria (PSB), and it may be conducive to increase the dissolution of insoluble phosphate in soils (Zhou et al. 2020). On the whole, the effect of biochar on the P availability in soils largely depended on pyrolysis temperature. The biochar produced at the temperature of 450 °C had the largest improvement on the Olsen-P and inorganic P in two soils. The effect of biochar on the availability of P in soils also depended on soil types and biomass feedstocks (Fig. 5). The results showed that the biochar had a more effect on the P availability in acidic soil. The correlation analysis showed that the available P in biochar-amended soils had a better correlation with the available P in the RB than the CB, and biochar exhibited a larger effect on the P availability in the Ultisol than the Alfisol (Fig. 5). The difference may due to the higher acidity and poor nutrients of the Ultisol versus the Alfisol. Therefore, soil types, biochar feedstocks, and pyrolysis temperatures should be considered comprehensively when applying biochar as soil amendments.

5 Conclusions

Our results demonstrated that the pyrolysis temperature had a significant effect on the availability of P in biochars and biochar-amended soils. The contents of total P and Olsen-P in biochar increased with the pyrolysis temperature. The canola stalk biochar had higher content of total P than the rice straw biochar. The addition of biochar would improve the availability of P in soils by adding available P directly into the soil. However, the amount and form of available P added were dependent on pyrolysis temperature and feedstock of biochar. Biochar significantly increased the content of total P, Olsen-P, H_2O-extractable P (only in Alfisol), and H_2SO_4-extractable P in soils. The pyrolysis temperature also affected the forms of inorganic P in biochar-treated soils, resulting in the increase of Al-P and Fe–P. The soils treated with biochar produced at the temperature of 450 °C had the largest increase of inorganic P content. The effects of biochar on soil pH and the availability of P were also influenced by soil type. The available P extracted by different extraction solutions in the Alfisol was higher than the Ultisol. The content of available P in biochar-amended soils was significantly correlated with the pH of biochar and biochar-amended soils. On the whole, the biochar produced at the temperature of 450 °C had the largest effect on the availability of P in soils. The selection of biochar in practice should consider the suitable pyrolysis temperature to obtain the better soil improvement.

Declarations

Conflict of interest The authors declare no competing interests.

References

Adhikari S, Gascó G, Méndez A, Surapaneni A, Jegatheesan V, Shah K, Paz-Ferreiro J (2019) Influence of pyrolysis parameters on phosphorus fractions of biosolids derived biochar. Sci Total Environ 695:133846. https://doi.org/10.1016/j.scitotenv.2019.133846

Ahmad M, Lee SS, Dou X, Mohan D, Sung JK, Yang JE, Ok YS (2012) Effects of pyrolysis temperature on soybean stover-and peanut shell-derived biochar properties and TCE adsorption in water. Biores Technol 118:536–544. https://doi.org/10.1016/j.biortech.2012.05.042

Bao SD (2000) Soil and agricultural chemistry analysis. Chinese Agriculture Press, Beijing

Blake L, Mercik S, Koerschens M, Moskal S, Poulton PR, Goulding KWT, Weigel A, Powlson DS (2000) Phosphorus content in soil, uptake by plants and balance in three European long-term field experiments. Nutr Cycl Agroecosyst 56(3):263–275. https://doi.org/10.1023/A:1009841603931

Boehm HP (1994) Some aspects of the surface chemistry of carbon blacks and other carbons. Carbon 32(5):759–769. https://doi.org/10.1016/0008-6223(94)90031-0

Chintala R, Schumacher TE, McDonald LM, Clay DE, Malo DD, Papiernik SK, Clay SA, Julson JL (2014) Phosphorus sorption and availability from biochars and soil/Biochar mixtures. CLEAN–Soil, Air, Water 42(5): 626–634. https://doi.org/10.1002/clen.201300089

Cole EJ, Zandvakili OR, Xing B, Hashemi M, Barker AV, Herbert SJ (2019) Effects of hardwood biochar on soil acidity, nutrient dynamics, and sweet corn productivity. Commun Soil Sci Plant Anal 50(14):1732–1742. https://doi.org/10.1080/00103624.2019.1632343

Cross AF, Schlesinger WH (1995) A literature review and evaluation of the Hedley fractionation: applications to the biogeochemical cycle of soil phosphorus in natural ecosystems. Geoderma 64:197–214. https://doi.org/10.1016/0016-7061(94)00023-4

da Silva CB, Fitzsimmons K (2016) The effect of pH on phosphorus availability and speciation in an aquaponics nutrient solution. Biores Technol 219:778–781. https://doi.org/10.1016/j.biortech.2016.08.079

de Figueiredo CC, Pinheiro TD, de Oliveira LEZ, de Araujo AS, Coser TR, Paz-Ferreiro J (2020) Direct and residual effect of biochar derived from biosolids on soil phosphorus pools: a four-year field assessment. Sci Total Environ 739:140013. https://doi.org/10.1007/s11368-011-0365-0

Dai Z, Zhang X, Tang C, Muhammad N, Wu J, Brookes PC, Xu J (2017) Potential role of biochars in decreasing soil acidification-a critical review. Sci Total Environ 581:601–611. https://doi.org/10.1016/j.scitotenv.2016.12.169

DeLuca TH, Gundale MJ, MacKenzie MD, Jones DL (2015) Biochar effects on soil nutrient transformations. Biochar for Environmental Management: Science, Technology and Implementation 2:421–454

Eduah JO, Nartey EK, Abekoe MK, Breuning-Madsen H, Andersen MN (2019) Phosphorus retention and availability in three contrasting soils amended with rice husk and corn cob biochar at varying pyrolysis temperatures. Geoderma 341:10–17. https://doi.org/10.1016/j.geoderma.2019.01.016

Figueiredo C, Lopes H, Coser T, Vale A, Busato J, Aguiar N, Novotny E, Canellas L (2018) Influence of pyrolysis temperature on chemical and physical properties of biochar from sewage sludge. Arch Argon Soil Sci 64(6):881–889. https://doi.org/10.1080/03650340.2017.1407870

Gao S, DeLuca TH (2018) Wood biochar impacts soil phosphorus dynamics and microbial communities in organically-managed croplands. Soil Biol Biochem 126:144–150. https://doi.org/10.1016/j.soilbio.2018.09.002

Gao S, DeLuca TH, Cleveland CC (2019) Biochar additions alter phosphorus and nitrogen availability in agricultural ecosystems: A meta-analysis. Sci Total Environ 654:463–472. https://doi.org/10.1016/j.scitotenv.2018.11.124

Gaskin JW, Steiner C, Harris K, Das KC, Bibens B (2008) Effect of low-temperature pyrolysis conditions on biochar for agricultural use. Trans ASABE 51(6): 2061–2069. https://doi.org/10.13031/2013.25409

Gérard F (2016) Clay minerals, iron/aluminum oxides, and their contribution to phosphate sorption in soils—a myth revisited. Geoderma 262:213–226. https://doi.org/10.1016/j.geoderma.2015.08.036

Glaser B, Lehmann J, Zech W (2002) Ameliorating physical and chemical properties of highly weathered soils in the tropics with charcoal–a review. Biol Fertil Soils 35(4):219–230. https://doi.org/10.1007/s00374-002-0466-4

Glaser B, Lehr VI (2019) Biochar effects on phosphorus availability in agricultural soils: a meta-analysis. Sci Rep 9(1):1–9. https://doi.org/10.1038/s41598-019-45693-z

Gustafsson JP, Mwamila LB, Kergoat K (2012) The pH dependence of phosphate sorption and desorption in Swedish agricultural soils. Geoderma 189:304–311. https://doi.org/10.1016/j.geoderma.2012.05.014

Harrington BA, Humphreys G (2004) Plant accessible phosphorus as a discriminator of native vegetation in the upper Blue Mountains. In Supersoil: 3rd Australian New Zealand Soils Conference, p 5–9

Hass A, Gonzalez JM, Lima IM, Godwin HW, Halvorson JJ, Boyer DG (2012) Chicken manure biochar as liming and nutrient source for acid Appalachian soil. J Environ Qual 41(4):1096–1106. https://doi.org/10.2134/jeq2011.0124

Hedley M, Stewart JWB, Chauhan B (1982) Changes in inorganic and organic soil phosphorus fractions induced by cultivation practices and by laboratory incubations. Soil Sci Soc Am J 46(5):970–976. https://doi.org/10.2136/sssaj1982.03615995004600050017x

Hollister CC, Bisogni JJ, Lehmann J (2013) Ammonium, nitrate, and phosphate sorption to and solute leaching from biochars prepared from corn stover (*Zea mays* L.) and oak wood (*Quercus* spp). J Environ Qual 42(1): 137–144. https://doi.org/10.2134/jeq2012.0033

Hong C, Lu S (2018) Does biochar affect the availability and chemical fractionation of phosphate in soils? Environ Sci Pollut Res 25(9):8725–8734. https://doi.org/10.1007/s11356-018-1219-8

Kameyama K, Miyamoto T, Shiono T, Shinogi Y (2012) Influence of sugarcane bagasse-derived biochar application on nitrate leaching in calcaric dark red soil. J Environ Qual 41(4):1131–1137. https://doi.org/10.2134/jeq2010.0453

Kim JA, Vijayaraghavan K, Reddy HK, Yun YS (2018) A phosphorus-enriched biochar fertilizer from bio-fermentation waste: a potential alternative source for phosphorus fertilizers. J Clean Prod 196:163–171. https://doi.org/10.1016/j.jclepro.2018.06.004

Knicker H (2007) How does fire affect the nature and stability of soil organic nitrogen and carbon? A Review Biogeochemistry 85(1):91–118. https://doi.org/10.1007/s10533-007-9104-4

Li H, Li Y, Xu Y, Lu X (2020) Biochar phosphorus fertilizer effects on soil phosphorus availability. Chemosphere 244-25471. https://doi.org/10.1016/j.chemosphere.2019.125471

Liu L, Tan Z, Gong H, Huang Q (2018) Migration and transformation mechanisms of nutrient elements (N, P, K) within biochar in straw–biochar–soil–plant systems: a review. ACS Sustain Chem Eng 7(1):22–32. https://doi.org/10.1021/acssuschemeng.8b04253

Ma J, He P, Xu X, He W, Liu Y, Yang F, Chen F, Li S, Tu S, Jin J, Johnston AM, Zhou W (2016) Temporal and spatial changes in soil available phosphorus in China (1990–2012). Field Crop Res 192:13–20. https://doi.org/10.1016/j.fcr.2016.04.006

Mehlich A (1978) New extractant for soil test evaluation of phosphorus, potassium, magnesium, calcium, sodium, manganese and zinc. Commun Soil Sci Plant Anal 9(6):477–492. https://doi.org/10.1080/00103627809366824

Morales MM, Comerford N, Guerrini IA, Falcão NPS, Reeves JB (2013) Sorption and desorption of phosphate on biochar and biochar–soil mixtures. Soil Use Manag 29(3):306–314. https://doi.org/10.1111/sum.12047

Murphy JAMES, Riley JP (1962) A modified single solution method for the determination of phosphate in natural waters. Anal Chim Acta 27:31–36. https://doi.org/10.1016/S0003-2670(00)88444-5

Oladele SO, Adeyemo AJ, Awodun MA (2019) Influence of rice husk biochar and inorganic fertilizer on soil nutrients availability and rain-fed rice yield in two contrasting soils. Geoderma 336:1–11. https://doi.org/10.1016/j.geoderma.2018.08.025

Parvage MM, Ulén B, Eriksson J, Strock J, Kirchmann H (2013) Phosphorus availability in soils amended with wheat residue char. Biol Fertil Soils 49(2):245–250. https://doi.org/10.1007/s00374-012-0746-6

Peng XY, Ye LL, Wang CH, Zhou H, Sun B (2011) Temperature- and duration-dependent rice straw-derived biochar: characteristics and its effects on soil properties of an Ultisol in southern China. Soil Tillage Res 112(2):159–166. https://doi.org/10.1016/j.still.2011.01.002

Peng Y, Sun Y, Fan B, Zhang S, Bolan NS, Chen Q, Tsang DC (2021a) Fe/Al (hydr) oxides engineered biochar for reducing phosphorus leaching from a fertile calcareous soil. J Clean Prod 279-123877. https://doi.org/10.1016/j.jclepro.2020.123877

Peng Y, Sun Y, Hanif A, Shang J, Shen Z, Hou D, Zhou Y, Chen Q, Ok YS, Tsang DC (2021b) Design and fabrication of exfoliated Mg/Al layered double hydroxides on biochar support. J Clean Prod 289-125142. https://doi.org/10.1016/j.jclepro.2020.125142

Qian TT, Jiang H (2014) Migration of phosphorus in sewage sludge during different thermal treatment processes. ACS Sustain Chem Eng 2:1411–1419. https://doi.org/10.1021/sc400476j

Santos SRD, Lustosa Filho JF, Vergütz L, Melo LCA (2019) Biochar association with phosphate fertilizer and its influence on phosphorus use efficiency by maize. Cienc Agrotecnol 43. https://doi.org/10.1590/1413-7054201943025718

Schneider F, Haderlein SB (2016) Potential effects of biochar on the availability of phosphorus—mechanistic insights. Geoderma 277:83–90. https://doi.org/10.1016/j.geoderma.2016.05.007

Shen J, Yuan L, Zhang J, Li H, Bai Z, Chen X, Zhang W, Zhang F (2011) Phosphorus dynamics: from soil to plant. Plant Physiol 156(3):997–1005. https://doi.org/10.1104/pp.111.175232

Solaiman ZM, Abbott LK, Murphy DV (2019) Biochar phosphorus concentration dictates mycorrhizal colonisation, plant growth and soil phosphorus cycling. Sci Rep 9(1):1–11. https://doi.org/10.9734/irjpac/2020/v21i930193

Sun K, Qiu M, Han L, Jin J, Wang Z, Pan Z, Xing B (2018) Speciation of phosphorus in plant-and manure-derived biochars and its dissolution under various aqueous conditions. Sci Total Environ 634:1300–1307. https://doi.org/10.1016/j.scitotenv.2018.04.099

Uchimiya M, Wartelle LH, Klasson KT, Fortier CA, Lima IM (2011) Influence of pyrolysis temperature on biochar property and function as a heavy metal sorbent in soil. J Agric Food Chem 59(6):2501–2510. https://doi.org/10.1021/jf104206c

Uzoma KC, Inoue M, Andry H, Zahoor A, Nishihara E (2011) Influence of biochar application on sandy soil hydraulic properties and nutrient retention. J Food Agric Environ 9(3/4 part 2): 1137–1143

Wang T, Camps-Arbestain M, Hedley M (2014) The fate of phosphorus of ash-rich biochars in a soil-plant system. Plant Soil 375(1–2):61–74. https://doi.org/10.1007/s11104-013-1938-z

Wang Z, Guo H, Shen F, Yang G, Zhang Y, Zeng Y, Wang L, Xiao H, Deng S (2015) Biochar produced from oak sawdust by Lanthanum (La)-involved pyrolysis for adsorption of ammonium (NH_4^+), nitrate (NO_3^-), and phosphate (PO_4^{3-}). Chemosphere 119:646–653. https://doi.org/10.1016/j.chemosphere.2014.07.084

Wei L, Xu G, Shao H, Sun J, Chang SX (2013) Regulating environmental factors of nutrients release from wheat straw biochar for sustainable agriculture. CLEAN–Soil, Air, Water 41(7): 697–701. https://doi.org/10.1002/clen.201200347

Xu N, Tan G, Wang H, Gai X (2016) Effect of biochar additions to soil on nitrogen leaching, microbial biomass and bacterial community structure. Eur J Soil Biol 74:1–8. https://doi.org/10.1016/j.ejsobi.2016.02.004

Yang F, Zhang S, Sun Y, Tsang DC, Cheng K, Ok YS (2019) Assembling biochar with various layered double hydroxides for enhancement of phosphorus recovery. J Hazard Mater 365:665–673. https://doi.org/10.1016/j.jhazmat.2018.11.047

Yang L, Wu Y, Wang Y, An W, Jin J, Sun K, Wang X (2020) Effects of biochar addition on the abundance, speciation, availability, and leaching loss of soil phosphorus. Sci Total Environ 143657. https://doi.org/10.1016/j.scitotenv.2020.143657

Zhang H, Chen C, Gray EM, Boyd SE, Yang H, Zhang D (2016) Roles of biochar in improving phosphorus availability in soils: a phosphate adsorbent and a source of available phosphorus. Geoderma 276:1–6. https://doi.org/10.1016/j.geoderma.2016.04.020

Zheng H, Wang Z, Deng X, Zhao J, Luo Y, Novak J, Herbert S, Xing B (2013) Characteristics and nutrient values of biochars produced from giant reed at different temperatures. Biores Technol 130:463–471. https://doi.org/10.1016/j.biortech.2012.12.044

Zhou C, Heal K, Tigabu M, Xia L, Hu H, Yin D, Ma X (2020) Biochar addition to forest plantation soil enhances phosphorus availability and soil bacterial community diversity. For Ecol Manage 455:117635. https://doi.org/10.1016/j.foreco.2019.117635